Positive Pion Production by Polarized X Rays between 227 and 373 MeV*

R. C. Smith† AND R. F. Mozley

High-Energy Physics Laboratory, Stanford University, Stanford, California

(Received 28 January 1963)

Measurements have been made of the ratio of the π^+ photoproduction cross sections at right angles to and along the electric field vector. Data have been taken at 45°, 90°, and 135° at energies of 227, 240, 342, and 373 MeV. A comparison of the data with the predictions of a phenomenological analysis using only S and P waves shows less than 0.1% chance of obtaining such results without the inclusion of higher angular momenta, and hence, demonstrates even more convincingly the need for a meson current term which has been indicated by other measurements. A comparison is made with the relativistic dispersion relations of McKinley which include an approximation for the γ, ρ, π coupling. At the resonance energy our polarization asymmetry is insensitive to this coupling and is in good agreement with the McKinley prediction. At lower energy the agreement is not as good but our data seem to substantiate the need for a negative γ, ρ, π coupling constant.

I. INTRODUCTION

EVEN in the energy region of the first resonance and below, the quantitative agreement of π^+ photoproduction measurements with calculated cross sections has been disappointingly bad. The use of polarized x rays to study photoproduction in this region allows a measurement of the cross section perpendicular to and parallel to the electric field vector ($\sigma_\perp$ and $\sigma_{\shortparallel}$) and permits the isolation of some terms in the cross section, thus, possibly aiding in understanding the theoretical difficulties. For example, the meson current term and all of its interference terms are entirely contained in $\sigma_{\shortparallel}$.

The work below describes the use of a beam of polarized bremsstrahlung to study π^+ photoproduction at 45°, 90°, and 135° and at photon laboratory energies of 227, 240, 342, and 373 MeV. No measurement has been made of the polarization and a calculated value is used in evaluating the data.

Angular distribution measurements of low-energy π^+ photoproduction[1-3] have shown the desirability of a meson current term and general theoretical arguments require its presence. However, the use of polarized x rays has allowed a statistically very convincing phenomenological demonstration of its existence since it causes very large qualitative changes in the asymmetry $(\sigma_\perp - \sigma_{\shortparallel})/(\sigma_\perp + \sigma_{\shortparallel})$. In addition, the measurements are compared with the dispersion relations of McKinley[4] which are similar to those of CGLN[5] but avoid a $1/M$ expansion and include terms for the γ, ρ, π coupling, thus providing an additional parameter (Λ) for at-

tempting to fit the experimental data. In the resonance region our polarization asymmetry is insensitive to this coupling and is in good agreement with the general predictions of the theory. At the lower energy the agreement is not as good but our data appear to substantiate[4,6] the need for a negative γ, ρ, π coupling constant.

II. PRODUCTION OF POLARIZED BREMSSTRAHLUNG

Calculations of May,[7] using a relativistic small-angle approximation, give the following results for dN_t (photons polarized perpendicular to the production plane) and dN_r (for photons polarized parallel to the production plane):

$$dN_t = 2\frac{\bar{\Phi}}{\pi}\frac{d\xi}{\xi}\frac{d\varphi_0 dx_0}{(1+x_0)^2}$$

$$\times \left\{ \left[1 - \xi + \frac{\xi^2}{2}\right] \ln\frac{1+x_0}{f} - (1-\xi) - \frac{\xi^2}{4} \right\}, \quad (1)$$

$$dN_r = 2\frac{\bar{\Phi}}{\pi}\frac{d\xi}{\xi}\frac{d\varphi_0 dx_0}{(1+x_0)^2}\left\{\left[1 - \xi + \frac{\xi^2}{2} - 4(1-\xi)\frac{x_0}{(1+x_0)^2}\right]\right.$$

$$\left.\times\ln\frac{1+x_0}{f} - \frac{\xi^2}{4} + (1-\xi)\left[1 - 2\left(\frac{1-x_0}{1+x_0}\right)^2\right]\right\}, \quad (2)$$

where $x_0 = E_0^2 \sin^2\theta_0$, $\xi = k/E_0$, $f = Z^{1/3}/108$, $\bar{\Phi} = Z^2 e^4/137$, E_0 is the energy of the incident electron, θ_0 is the bremsstrahlung angle, k is the photon energy, and Z is the atomic number of the radiator nucleus. All energies and momenta are in units of the rest energy of the electron and the velocity of light is set equal to unity.

These formulas are derived using an extreme relativistic Born approximation and an approximate screening potential but without Coulomb corrections. A comparison made with the more accurate Olsen and Maximon[8] formulas shows a negligible difference from

¹ J. H. Malmberg and C. S. Robinson, Phys. Rev. 109, 158 (1958).
² A. Lazarus, W. K. H. Panofsky, and F. Tangherlini, Phys. Rev. 113, 1330 (1959).
³ E. A. Knapp, R. W. Kenney, and V. Perez-Mendez, Phys. Rev. 114, 605 (1959).
⁴ J. M. McKinley, Technical Report No. 38, Physics Dept., University of Illinois, Champaign-Urbana, Illinois (unpublished).
⁵ G. F. Chew, M. L. Goldberger, E. F. Low, and Y. Nambu, Phys. Rev. 106, 1345 (1957); referred to as CGLN.

⁶ C. S. Robinson, P. M. Baum, L. Criegee, and J. M. McKinley, Phys. Rev. Letters 9, 349 (1962).
⁷ M. M. May, Phys. Rev. 84, 265 (1951).
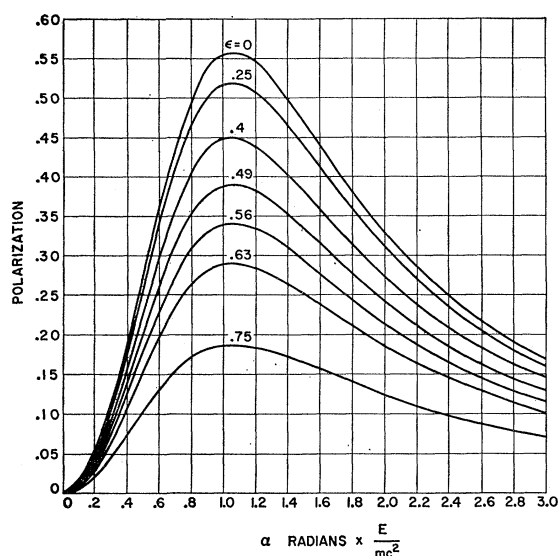⁸ H. Olsen and L. C. Maximon, Phys. Rev. 114, 887 (1959).

Fig. 1. May's calculated values of polarization $\xi = k/E_0$.

these predictions ($<1\%$, in the polarization prediction under the circumstances of our experiment).

Of more importance is the approximation of assuming that the polarization and distribution of electron-electron bremsstrahlung is the same as that of nuclear bremsstrahlung, but fortunately a recent calculation by Scofield[9] has shown that there is no major difference.

May's predictions of polarization $P = (dN_t - dN_r)/(dN_t + dN_r)$ are shown in Fig. 1. It can be seen that the polarization reaches a maximum at an angle of mc^2/E_0 and is larger for smaller values of $\xi = k/E_0$. These theoretically predicted values of the polarization must be modified to take multiple scattering, beam size, and angular divergence into consideration. The effect of multiple scattering for an experiment using polarized bremsstrahlung has been discussed by Taylor and Mozley,[10] and their method of handling this problem has been used in the present work. Of immediate concern is the modification of May's polarization versus angle curves due to multiple scattering. The resulting modifications are shown in Fig. 2. As described by Taylor and Mozley, the effect of multiple scattering on polarization is to lessen the polarization and increase somewhat the angle of maximum polarization. In addition, the effects of the collimator aperture must also be folded into the polarization curve, Fig. 2, to obtain the polarization values used in the present measurements, Fig. 3.

III. PHOTOPRODUCTION OF PIONS

It is well known that a retardation term is necessary in charged pion photoproduction. Many photoproduction measurements indicate the desirability of a re-

tardation term in the photoproduction matrix element for positive pions. In particular, the measurements of Malmberg and Robinson[1] have shown that it is statistically difficult to fit their data without momenta higher than S and P waves. At high energies very convincing measurements[11] show that the angular distribution of charged pion production can be qualitatively explained as dominated by such a term. However, only photons polarized in the plane of production contribute to the retardation term and, hence, the use of polarized bremsstrahlung provides a more straightforward method for establishing the existence of this term with greater statistical significance than that provided by ordinary angular distribution measurements. If one repeats the type of argument used by Malmberg and Robinson, pointing out that if no retardation term is present it is unlikely that partial waves greater than P wave are important at low energies for the photoproduction of charged pions (as indicated by scattering data and by general theoretical arguments regarding the distance of the interaction), one requires data at only two angles to obtain significant information. On the other hand, an angular distribution analysis requires measurements at a minimum of four angles. If, in addition, the possibility of D wave is included, four measurements are required in an experiment with polarized x rays compared with the six required by an angular distribution analysis of data taken with an unpolarized beam. Our data have been analyzed with
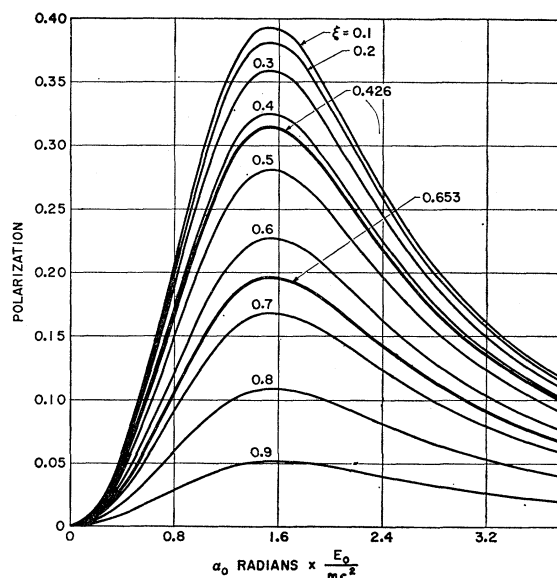

Fig. 2. Calculated values of polarization with multiple scattering by 20.3 mg/cm² aluminum radiator included.

[11] M. Beneventano, G. Finocchiaro, R. Finzi, L. Mezzetti, L. Paoluzzi, and C. Schaerf, Nuovo Cimento 17, 274 (1960). J. H. Boyden and R. L. Walker, in *Proceedings of the 1960 International Conference on High-Energy Physics at Rochester*, edited by E. C. G. Sudarshan, J. H. Tinlot, and A. C. Melissinos (University of Rochester Press, Rochester, New York, 1960), p. 17.

[9] J. Scofield (private communication).
[10] R. E. Taylor and R. F. Mozley, Phys. Rev. 117, 835 (1960).

S and P waves alone, and with S, P, and a small amount of D wave (which requires three measurements).

Of particular importance to this measurement is the additional fact that only production ratios along and at right angles to the electric field vector must be measured and not the cross section itself. Cross-section data are required, but the data of others taken with unpolarized bremsstrahlung can be used. It can be shown that the errors of the unpolarized data propagate with less emphasis than those of the polarization asymmetry measurements, and thus the final accuracy is governed primarily by the errors and counting statistics of this experiment.

The approach used to "establish" the existence of the retardation term is to make a comparison of the data with a phenomenological analysis assuming the presence of only a limited number of partial waves (S

and P; or S, P, and small D). It can be shown that the data do not fit such an analysis and that the character of the disagreement is similar to that predicted by the relativistic dispersion theory which does include such a term.

The phenomenological approach used in the following analysis is essentially the same as that used by Gell-Mann and Watson[12] and elaborated by Moravcsik.[13]

The general amplitude for photoproduction, including partial waves up to D wave, is given below. We use the notation of Moravcsik, where the amplitudes for a given reaction are labeled $E_{l_\pi\,2J}$ for an electric multipole and $M_{l_\pi\,2J}$ for a magnetic multipole. l_π is the total angular momentum of the outgoing pion and J is the total angular momentum of the system. If angular momentum states up to D wave are included, the scattering amplitude for photoproduction becomes

$$T = iE_{01}[\vec{\sigma}\cdot\hat{\epsilon}] + iM_{11}[(\vec{\sigma}\cdot\hat{k})(\hat{q}\cdot\hat{\epsilon}) - (\vec{\sigma}\cdot\hat{\epsilon})(\hat{q}\cdot\hat{k}) - i\hat{q}\cdot(\hat{k}\times\hat{\epsilon})] + iM_{13}[(\vec{\sigma}\cdot\hat{\epsilon})(\hat{q}\cdot\hat{k}) - (\vec{\sigma}\cdot\hat{k})(\hat{q}\cdot\hat{\epsilon}) - 2i\hat{q}\cdot(\hat{k}\times\hat{\epsilon})]$$
$$+ 3iE_{13}[(\vec{\sigma}\cdot\hat{\epsilon})(\hat{q}\cdot\hat{k}) + (\vec{\sigma}\cdot\hat{k})(\hat{q}\cdot\hat{\epsilon})] + 3iM_{23}[(\vec{\sigma}\cdot\hat{\epsilon}) - (\vec{\sigma}\cdot\hat{q})(\hat{q}\cdot\hat{\epsilon}) + 2(\vec{\sigma}\cdot\hat{k})(\hat{q}\cdot\hat{\epsilon})(\hat{q}\cdot\hat{k}) - 2(\vec{\sigma}\cdot\hat{\epsilon})(\hat{q}\cdot\hat{k})^2$$
$$- 2i(\hat{q}\cdot\hat{k})\hat{q}\cdot(\hat{k}\times\hat{\epsilon})] + iE_{23}[(\vec{\sigma}\cdot\hat{\epsilon}) - 3(\vec{\sigma}\cdot\hat{q})(\hat{q}\cdot\hat{\epsilon})] + 3iM_{25}[-(\vec{\sigma}\cdot\hat{\epsilon}) + (\vec{\sigma}\cdot\hat{q})(\hat{q}\cdot\hat{\epsilon}) + 2(\vec{\sigma}\cdot\hat{\epsilon})(\hat{q}\cdot\hat{k})^2$$
$$- 2(\vec{\sigma}\cdot\hat{k})(\hat{q}\cdot\hat{\epsilon})(\hat{q}\cdot\hat{k}) - 3i(\hat{q}\cdot\hat{k})\hat{q}\cdot(\hat{k}\times\hat{\epsilon})] + 3iE_{25}[-\tfrac{1}{2}(\vec{\sigma}\cdot\hat{\epsilon}) - (\vec{\sigma}\cdot\hat{q})(\hat{q}\cdot\hat{\epsilon}) + \tfrac{5}{2}(\vec{\sigma}\cdot\hat{\epsilon})(\hat{q}\cdot\hat{k})^2 + 5(\vec{\sigma}\cdot\hat{k})(\hat{q}\cdot\hat{\epsilon})(\hat{q}\cdot\hat{k})]. \quad (3)$$

All vectors shown are unit vectors; σ corresponds to the nucleon spin, q to pion momentum, k to photon momentum, and ϵ to the photon polarization. Averaging T^2 over the nucleon spin the cross section up to D wave is obtained:

$$\sigma = K\,\mathrm{Re}\{[|E_{01}|^2 + |M_{11}|^2 + \tfrac{5}{2}|M_{13}|^2 + \tfrac{9}{2}|E_{13}|^2 + \tfrac{9}{2}|M_{23}|^2 + \tfrac{5}{2}|E_{23}|^2 + \tfrac{9}{2}|M_{25}|^2 + (45/4)|E_{25}|^2 + 3(E_{01}{}^*M_{23})$$
$$- (E_{01}{}^*E_{23}) - 3(E_{01}{}^*M_{25}) - 6(E_{01}{}^*E_{25}) + (M_{11}{}^*M_{13}) + 3(M_{11}{}^*E_{13}) - 3(M_{13}{}^*E_{13}) + 3(M_{23}{}^*E_{23})$$
$$- 9(M_{23}{}^*M_{25}) - \tfrac{9}{2}(M_{23}{}^*E_{25}) - 3(E_{23}{}^*M_{25}) + (15/2)(E_{23}{}^*E_{25}) + \tfrac{9}{2}(M_{25}{}^*E_{25})]$$
$$+ \cos\theta[-4(E_{01}{}^*M_{11}) + 2(E_{01}{}^*M_{13}) + 6(E_{01}{}^*E_{13}) + 6(M_{11}{}^*M_{23}) - 2(M_{11}{}^*E_{23}) + 9(M_{11}{}^*M_{25}) + 18(M_{11}{}^*E_{25})$$
$$+ 12(M_{13}{}^*M_{23}) + 2(M_{13}{}^*E_{23}) + 18(M_{13}{}^*M_{25}) - 18(M_{13}{}^*E_{25}) + 18(E_{13}{}^*M_{23}) - 12(E_{13}{}^*E_{23})$$
$$- 18(E_{13}{}^*M_{25}) + 18(E_{13}{}^*E_{25})]$$
$$+ \cos^2\theta[-\tfrac{3}{2}|M_{13}|^2 + \tfrac{9}{2}|E_{13}|^2 + \tfrac{9}{2}|M_{23}|^2 - \tfrac{3}{2}|E_{23}|^2 + 27|M_{25}|^2 + (27/2)|E_{25}|^2 - 9(E_{01}{}^*M_{23}) + 3(E_{01}{}^*E_{23})$$
$$+ 9(E_{01}{}^*M_{25}) + 18(E_{01}{}^*E_{25}) - 3(M_{11}{}^*M_{13}) - 9(M_{11}{}^*E_{13}) + 9(M_{13}{}^*E_{13}) - 9(M_{23}{}^*E_{23}) + 81(M_{23}{}^*M_{25})$$
$$+ 81(M_{23}{}^*E_{25}) + 9(E_{23}{}^*M_{25}) - 63(E_{23}{}^*E_{25}) - 81(M_{25}{}^*E_{25})]$$
$$+ \cos^3\theta[-15(M_{11}{}^*M_{25}) - 30(M_{11}{}^*E_{25}) - 18(M_{13}{}^*M_{23}) - 12(M_{13}{}^*M_{25}) + 30(M_{13}{}^*E_{25}) - 36(E_{13}{}^*M_{23})$$
$$+ 18(E_{13}{}^*E_{23}) + 36(E_{13}{}^*M_{25}) + 18(E_{13}{}^*E_{25})]$$
$$+ \cos^4\theta[-(45/2)|M_{25}|^2 + (45/4)|E_{25}|^2 - 90(M_{23}{}^*M_{25}) - (225/2)(M_{23}{}^*E_{25}) + (135/2)(E_{23}{}^*E_{25})$$
$$+ (225/2)(M_{25}{}^*E_{25})]$$
$$+ \sin^2\theta\cos2\varphi[-\tfrac{3}{2}|M_{13}|^2 + \tfrac{9}{2}|E_{13}|^2 - \tfrac{9}{2}|M_{23}|^2 + \tfrac{3}{2}|E_{23}|^2 - \tfrac{9}{2}|M_{25}|^2 + 9|E_{25}|^2 - 3(E_{01}{}^*M_{23}) - 3(E_{01}{}^*E_{23})$$
$$+ 3(E_{01}{}^*M_{25}) - 3(E_{01}{}^*E_{25}) - 3(M_{11}{}^*M_{13}) + 3(M_{11}{}^*E_{13}) - 3(M_{13}{}^*E_{13}) - 3(M_{23}{}^*E_{23}) + 9(M_{23}{}^*M_{25})$$
$$+ \tfrac{9}{2}(M_{23}{}^*E_{25}) + 3(E_{23}{}^*M_{25}) + (21/2)(E_{23}{}^*E_{25}) - \tfrac{9}{2}(M_{25}{}^*E_{25})]$$
$$+ \sin^2\theta\cos\theta\cos2\varphi[-15(M_{11}{}^*M_{25}) + 15(M_{11}{}^*E_{25}) - 18(M_{13}{}^*M_{23}) - 12(M_{13}{}^*M_{25}) - 15(M_{13}{}^*E_{25})$$
$$- 18(E_{13}{}^*E_{23}) + 27(E_{13}{}^*E_{25})]$$
$$\sin^2\theta\cos^2\theta\cos2\varphi[-(45/2)|M_{25}|^2 + 45|E_{25}|^2 - 90(M_{23}{}^*M_{25}) + (45/2)(M_{23}{}^*E_{25})$$
$$- (135/2)(E_{23}{}^*E_{25}) - (45/2)(M_{25}{}^*E_{25})]\}, \quad (4)$$

where K includes phase-space factors and various constants and is independent of the model. This may be written in the form:

$$\sigma = A + B\cos\theta + C\cos^2\theta + D\cos^3\theta + E\cos^4\theta$$
$$+ (\alpha + \beta\cos\theta + \gamma\cos^2\theta)\sin^2\theta\cos2\varphi \quad (5)$$

or

$$\sigma = \sigma_0 + (\alpha + \beta\cos\theta + \gamma\cos^2\theta)\sin^2\theta\cos2\varphi, \quad (6)$$

[12] M. Gell-Mann and K. M. Watson, Ann. Rev. Nucl. Sci. 4, 241 (1954).
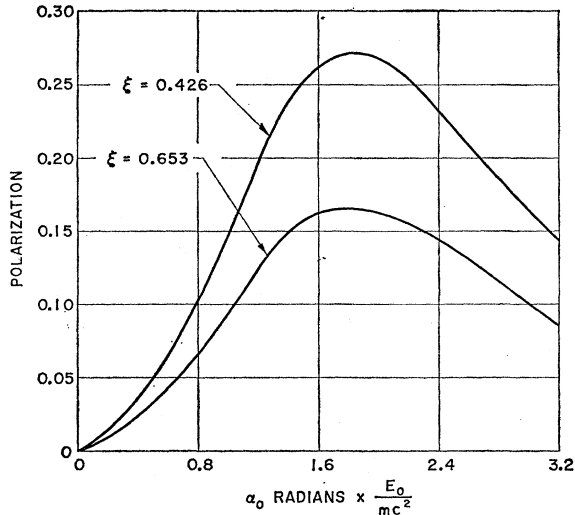[13] M. J. Moravcsik, Lectures given at Purdue University (1957).

FIG. 3. Calculated values of polarization with multiple scattering and $1.26 \times mc^2/E_0$ diameter aperture included.

where σ is the cross section averaged over nucleon spins, σ_0 is the cross section averaged over spin and over photon polarization, and the coefficients are combinations of the various multipole amplitudes. θ is the center-of-mass angle between the incoming photon direction and the outgoing pion, and φ is the angle between the photon polarization vector and the pion plane of emission. The cross section then can also be expressed as

$$\sigma_{\shortparallel} = \sigma_0 + (\alpha + \beta \cos\theta + \gamma \cos^2\theta) \sin^2\theta, \tag{7}$$

$$\sigma_{\perp} = \sigma_0 - (\alpha + \beta \cos\theta + \gamma \cos^2\theta) \sin^2\theta. \tag{8}$$

If only S and P waves contribute significantly in forming the photoproduction amplitude, Eq. (5) reduces to a simpler form:

$$\sigma = A + B \cos\theta + C \cos^2\theta + \alpha \sin^2\theta \cos 2\varphi, \tag{9}$$

which can be written as

$$\sigma = \sigma_0 + \alpha \sin^2\theta \cos 2\varphi. \tag{10}$$

If only S, P, and $D_{3/2}$ waves contribute significantly to the photoproduction amplitude, inspection of Eq. (4) shows that the photoproduction cross section has the form:

$$\sigma = \sigma_0 + (\alpha + \beta \cos\theta) \sin^2\theta \cos 2\varphi. \tag{11}$$

As another alternative, it may be assumed that S, P, $D_{3/2}$, and $D_{5/2}$ waves contribute to the photoproduction amplitude but that the D-wave amplitudes are small compared with S- and P-wave amplitudes. Imposing this last condition allows the neglect of all terms in the cross section which are the square of D-wave amplitudes. Inspection of Eq. (4) shows that, under the assumption of S-, P-, and a small amount of D-wave contribution, the cross section again takes the form shown in Eq. (11). Equations (10) and (11) are the equations of interest for the phenomenological analysis

of the data in this experiment. The use of these expressions for this analysis will be discussed below.

π^+ photoproduction is in disagreement with the predictions of the CGLN theory. A more accurate dispersion theoretical calculation has been done by McKinley[4] in a relativistic form without a $1/M$ expansion. The possibility of the participation of the ρ, a bi-pion resonance, has been suggested by several people[14–16] and McKinley includes the possible presence of the ρ in an approximate form. The free parameter coupling the γ, ρ, and π allows photoproduction to be much better fitted[4,6] but seems to have less effect on the asymmetry, $(\sigma_{\perp} - \sigma_{\shortparallel})/(\sigma_{\perp} + \sigma_{\shortparallel})$. The matrix element used is similar to that of CGLN and the resulting cross sections differ very little. The cross section is given by the following:

$$\sigma = 2e^2 f^2 (q/k) (\mathfrak{F}^- + \mathfrak{F}^0 + \mathfrak{F}_{\pi\pi}{}^0)^2. \tag{12}$$

Here the third term is due to the presence of the ρ and is treated in a manner similar to that of the De Tollis and Verganelakis.[15] It is expressed by the diagram of Fig. 4.

IV. EXPERIMENTAL EQUIPMENT

A beam of polarized bremsstrahlung was produced in a manner almost identical to that used by Taylor and Mozley. The radiator was a circular aluminum foil $\frac{1}{4}$ in. in diameter and 0.003 in. thick suspended in the unanalyzed beam of the Stanford Linear Accelerator by thin, 0.001-in., "Nichrome" wires. Its limited diameter reduced effects due to beam position variation while its small thickness was necessary to reduce multiple scattering. The beam was collimated 80 ft ahead of the radiator and focused on it in such a way as to avoid hitting the accelerator structure and causing intense background radiation (see Fig. 5). After striking the radiator the electron beam was deflected, its energy was measured, and it was then stopped inside of a 5-ft-thick concrete shielding wall (Fig. 6). The energy width of the beam was not controlled and could vary from between $\pm\frac{3}{4}\%$ to $\pm 2\%$.

A polarized portion of the bremsstrahlung beam was selected by steering the electron beam slightly just before it struck the radiator. The regions were chosen cyclically in quadrature about the direction of the undeflected electron beam in such a manner as to reduce steering errors (see Fig. 7). The angle, chosen to opti-
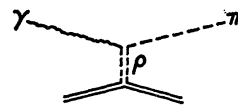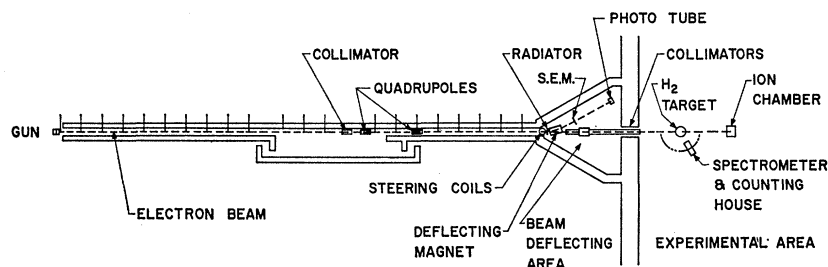

FIG. 4. Diagram illustrating the γ, ρ, π coupling.

[14] J. S. Ball, University of California Report, UCRL–9172 (unpublished); Phys. Rev. 124, 2014 (1961).
[15] B. De Tollis and A. Verganelakis, Phys. Rev. Letters 6, 371 (1961).
[16] M. Gourdin, D. Turie, and A. Martin, Nuovo Cimento 18, 933 (1960).

FIG. 5. Linear accelerator and arrangement of experimental equipment.

mize the data rate, gave polarizations of about 15–20%. The multiple scattering, angular divergence and beam size were measured by running the electron beam through a radiator $\frac{1}{2}$ the thickness of the one used for the experiment and then measuring the distribution of the electrons (undeflected by the energy analysis magnet) at the location of the collimator. This measurement was done by measuring the darkening of a glass plate and is described in reference 10. The effects of this distribution and also those of the collimators were folded into the polarization calculations as shown in Figs. 2 and 3.

No experimental determination of the polarization was made. Angular measurements of meson production were made cyclically at a constant bremsstrahlung energy and angle, and hence, at a constant polarization. Comparisons requiring a knowledge of the value of the polarization were obtained using a calculated value, and hence, are dependent upon May's polarization predictions and our handling of the electron beam and multiple scattering.

The equipment for production and detection of pions consisted essentially of a liquid-hydrogen target, a spectrometer, and associated electronic equipment. The liquid-hydrogen target system consisted of two separate 10-in.-long$\times$1$\frac{1}{2}$-in.-diam cylindrical targets suspended one above the other and fed by condensers immersed in a liquid-hydrogen reservoir. The targets were made of 0.002-in. stainless steel and then plated with 0.0005-

in. nickel plating. The two identical targets with separate transfer systems were mounted on a bellows system in a vacuum chamber which allowed either one or the other of the two targets to be placed in the beam line. In this experiment only one target was full and it was replaced by the other which was empty when an empty target background run was to be taken.

The liquid-hydrogen target was mounted in the beam line and centered in order to be at the focal point of the spectrometer (Fig. 8). The spectrometer consisted of a 30-in. radius large aperture (0.017 sr) analyzing magnet, placed on a shielding box made of 12-in.-thick steel plates. The whole spectrometer assembly could be rotated about the liquid-hydrogen target allowing measurements to be made at any polar angle from 0° to 180°. The magnet was calibrated by "floating wire" measurements[17] of the trajectories in the magnetic field and these calibrations were checked by calibration runs made directly with an electron beam. These two methods of calibration were in good agreement. The measurements provide a curve of magnet current versus momentum and the magnet resolution was found to give a $\Delta p/p$ of $\pm$ (4%), where p is the momentum of the particle being analyzed.

The pions were detected by counting the electrons from the decay chain $\pi \rightarrow \mu \rightarrow e$. Two (or three) plastic scintillators (10 in.$\times$4 in.$\times$3 in. thick), placed inside the shielding box, were covered with an appropriate thickness of absorber to stop the pi mesons when

FIG. 6. Equipment for the production of polarized bremsstrahlung.
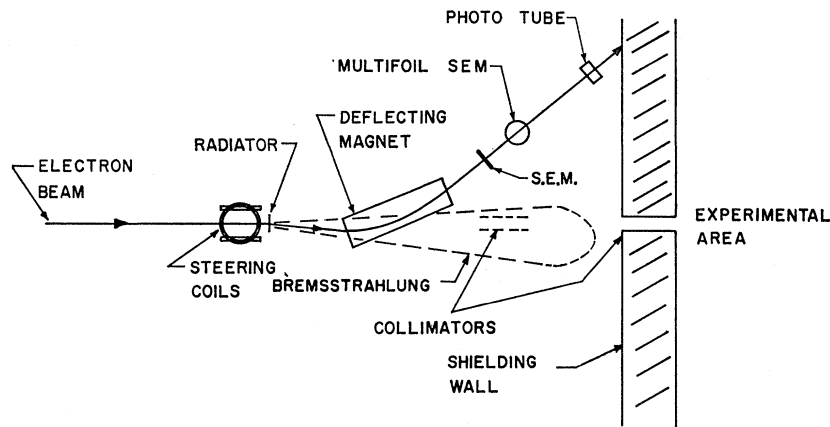
[17] L. Cranberg, U. S. Atomic Energy Commission Document, AECU 1670, 1951 (unpublished).
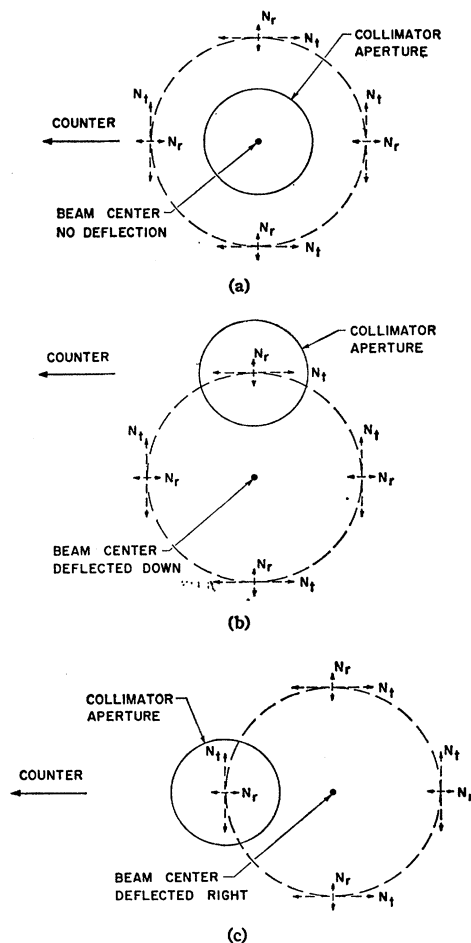
FIG. 7. Schematic diagram showing how the desired region of bremsstrahlung is selected by the use of steering coils and collimator. (a) Beam not deflected, (b) beam deflected down, and (c) beam deflected right.

halfway through the scintillator. The magnet selected the momentum of the pions, while the absorber thickness was a rough check on this momentum selection. The electron accelerator pulses sixty times per second with a beam pulse 0.9 μsec long and the counters selected particles which lost sufficient energy in the plastic scintillator during a 6.6-μsec period after the beam pulse. The particles detected in the scintillator were counted if they decayed during times defined by either of two "gates," the first of which was 2.2 μsec long starting 1.5 μsec after the start of the beam pulse, while the second was 4.4 μsec long starting immediately after the end of the first gate. This allowed a check that the particles being counted were mu mesons, since a particle of 2.2-μsec mean life would have two times as many counts in gate 1 as in gate 2, whereas, a relatively constant background would have half as many counts in gate 1 as in gate 2. A third gate, double the time of gates 1 and 2 combined, was delayed approximately 13 μsec after the beam pulse to measure the relatively constant background and this was subtracted. In addition, background subtractions were made using data taken with an empty target and with the 0.003 in. aluminum radiator foil removed.

The plastic scintillators were connected by means of Lucite light pipes to RCA 6810A multiplier phototubes. These phototubes were covered with a 0.050-in.-thick "Mumetal" and a 0.025-in.-thick "Nicoloi" magnetic shield which was surrounded by a 0.25-in.-thick soft iron pipe. This magnetic shielding was tested and found to be able to reduce a 75 G field, the maximum present, to less than 0.2 G, a permissible level for the 6810A phototube. The pulse from the phototube was passed through a discriminator and into a selector circuit which separated the pulses from the phototubes by means of gate circuits and, in addition, synchronized the switching of the polarization changing steering coils with a switching of the storage scalers in which the data were recorded. When the beam was deflected up or down (Fig. 7), the collimator would pass a polarized beam and one group of scalers would record $\eta(N_t\sigma_{11}+N_r\sigma_\perp)$ counts. σ_{11} refers to the cross section for meson production with the polarization of the photon in the plane of production $(\varphi=0)$, $\sigma_\perp$ refers to the cross section with the polarization perpendicular to that plane. $(\varphi=\pi/2)$, and η is a constant containing such factors as the efficiency of the counter, the solid angle accepted by the counter, the photon energy range corresponding to the interval of pion energies accepted by the counter, etc. When the beam was deflected right or left, a second set of scalers would record $\eta(N_t\sigma_\perp+N_r\sigma_{11})$ counts. Thus, by making a complete cycle of the deflected beam, the following ratio could be measured:

$$R=\frac{\text{Number of counts in left+right position}}{\text{Number of counts in up+down position}}$$

(this R is $1/R$ in reference 10), or

$$R=\frac{N_t\sigma_\perp+N_r\sigma_{11}}{N_t\sigma_{11}+N_r\sigma_\perp}. \qquad (13)$$

V. ERRORS AND BACKGROUNDS

Of fundamental importance in reducing the systematic errors associated with the experiment is the fact that only ratios of meson yields were measured. As a result, no calibration of the efficiency of the counting equipment, absolute beam intensity, or magnet solid angle was required. The ratio data were taken a large number of times ($\sim$1000) by the use of automatic cycling and recording equipment and, thus, the effects of drifts in counter efficiency can be neglected. Since an ion chamber was used to measure the beam intensity, saturation effects might be expected. However, over regions of intensity of approximately 10–1, such effects were less than 1%.

A possible source of error is the measurement of the

"no radiator" background since in this case no ionization chamber measurement of the beam is possible. During these runs the deflected electron beam was measured by a secondary emission monitor and compared to similar measurements with the radiator present. Errors in such normalization could be as large as 10%. With regard to this it is important that the measurement of ratios reduced such error contributions to the final data. For example, let $R_c = (x-b_x)/(y-b_y)$ be a ratio which has been formed by measuring x and y and subtracting a background b_x and b_y. Let R_v be the same ratio uncorrected. The fractional change introduced by the background correction to the ratio is $(R_c-R_v)/R_c \simeq (R_c-R_v)/R_v \simeq b_y/y - b_x/x$. To the extent that the fractional background corrections are equal, no error is introduced by ignoring the background correction. If, as seems possible in the subtraction of the background from unpolarized x rays, the background is constant in size for both polarizations, the relation becomes $R = (x-b)/(y-b)$ and

$$\Delta R/R = [b(x-y)/(x-b)(y-b)](\Delta b/b).$$

For a typical ratio of $R=1.2$ a 10% background with a 10% error in the background introduces only a 0.2% error in R.

Checks were made that there were no hidden biases in the apparatus which would produce a ratio different from unity for unpolarized x rays. A measurement was made at a meson production angle $\theta=180°$ where the ratio should be unity regardless of the polarization. The ratio obtained was 1.014 ± 0.034. A second check was made by cycling the deflection of the electron beam in such a manner that the enhanced polarization was at
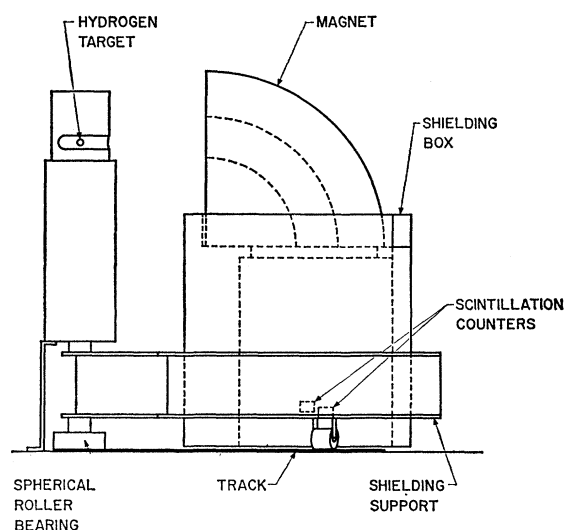

FIG. 8. Side view of equipment used for the detection of positive pions.

a 45° angle to the plane of meson production. The ratio measured in this case was 0.985 ± 0.032.

The measurement of multiple scattering was made only once during this experiment. The accelerator operating conditions were reproduced accurately from run to run and the distribution obtained agreed closely with measurements made under quite different operating conditions.[18] Hence, the value of the calculated polarization is estimated not to vary more than $\pm1\%$ between runs.

These sources of error are not included in the error estimates since they are not comparable to those due to counting statistics.

VI. RESULTS AND DISCUSSION

It was shown in the above section that by using the automatic cycling system which selects the appropriate region of polarization from the photon beam, the data obtained can be expressed in a ratio, Eq. (13). Since it can be shown that

$$(R-1)/(R+1) = P(\sigma_\perp - \sigma_{||})/(\sigma_\perp + \sigma_{||}), \qquad (14)$$

we quote the results of our measurements in these terms in Table I. This has the advantage of making errors due to our polarization estimates more readily identifiable.

Consider first the assumption that only S and P waves contribute to the photoproduction amplitude. Under this assumption, the cross section can be expressed as

$$\sigma = \sigma_0 + \alpha \sin^2\theta \cos 2\varphi. \qquad (10)$$

When $\varphi=0$, we have

$$\sigma_{||} = \sigma_0 + \alpha \sin^2\theta, \qquad (15)$$

TABLE I. Measured values of $(R-1)/(R+1)$, calculated values of polarization P, and derived values of $(\sigma_\perp - \sigma_{||})/(\sigma_\perp + \sigma_{||})$ at 227, 240, 342, 373 MeV. Average values for the combined data of 227 and 240 MeV are given as 234 MeV and for 342 and 373 as 359-MeV data.

$h\nu$ (MeV)	θ	$(R-1)/(R+1)$	P	$(\sigma_\perp - \sigma_{||})/(\sigma_\perp + \sigma_{||})$
227.3	45°	0.055±0.013	0.259	0.212±0.052
	90°	0.057±0.013		0.219±0.048
	135°	0.032±0.013		0.123±0.049
239.7	45°	0.055±0.016	0.250	0.221±0.063
	90°	0.037±0.014		0.148±0.058
	135°	0.003±0.017		0.010±0.067
234.4	45°	0.055±0.010	0.254	0.217±0.040
	90°	0.049±0.010		0.109±0.037
	135°	0.021±0.010		0.083±0.039
342.4	45°	0.099±0.013	0.172	0.574±0.076
	90°	0.114±0.017		0.664±0.098
	135°	0.059±0.015		0.342±0.085
373.0	45°	0.123±0.019	0.146	0.841±0.132
	90°	0.098±0.024		0.671±0.164
	135°	0.060±0.025		0.409±0.170
358.9	45°	0.106±0.011	0.158	0.674±0.068
	90°	0.109±0.014		0.689±0.088
	135°	0.059±0.013		0.376±0.081

---

[18] Darrell Drickey (private communication).
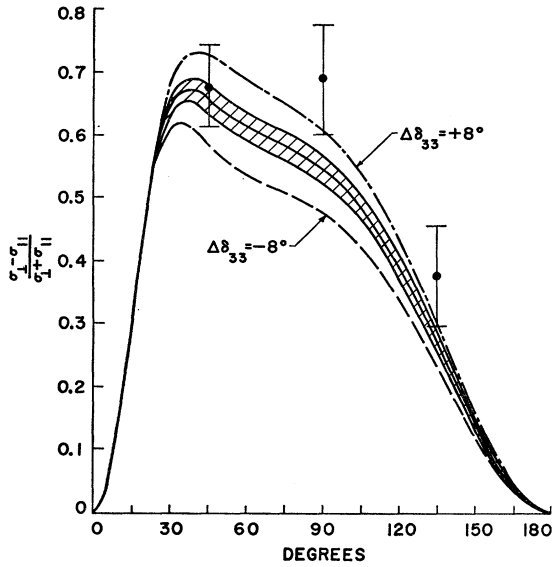
FIG. 9. Comparison of theoretical and measured values of $(\sigma_\perp - \sigma_{\shortparallel})/(\sigma_\perp + \sigma_{\shortparallel})$ at 359 MeV. In all curves $\Lambda = 0$. The central band encompasses the effects of varying all of the small phases individually by $\pm 2°$ from the central values given in Table V. Curves are also given for a $\pm 8°$ variation of the δ_{33} phase shift.

and when $\varphi = \pi/2$

$$\sigma_\perp = \sigma_0 - \alpha \sin^2\theta. \qquad (16)$$

Thus,

$$\sigma_\perp/\sigma_{\shortparallel} = (\sigma_0 - \alpha \sin^2\theta)/(\sigma_0 + \alpha \sin^2\theta). \qquad (17)$$

By introducing the photon polarization

$$P = (N_t - N_r)/(N_t + N_r), \qquad (18)$$

and using Eqs. (10) and (13), the following relationship can be formed:

$$P\alpha = \frac{-\sigma_0(\theta)}{\sin^2\theta}\left(\frac{R-1}{R+1}\right). \qquad (19)$$

For a given incident photon energy and polarization, $P\alpha$ is a constant, since the polarization and the constant α depend only on the photon energy. Thus measurements of R, knowing $\sigma_0(\theta)$, at different angles should give the same $P\alpha$ values if the assumptions of no retardation term and only S- and P-wave contributions are valid.

TABLE II. Measured values of $[-\sigma_0(\theta)/\sin^2\theta](R-1)/(R+1)$ at 342 and 373 MeV. These values should be independent of angle if only S and P waves are present.

	$\dfrac{-\sigma_0(\theta)}{\sin^2\theta}\left(\dfrac{R-1}{R+1}\right)_{k=342\ \mathrm{MeV}}$ (μb/sr)	$\dfrac{-\sigma_0(\theta)}{\sin^2\theta}\left(\dfrac{R-1}{R+1}\right)_{k=373\ \mathrm{MeV}}$ (μb/sr)
45°	2.71±0.39	2.92±0.37
90°	1.85±0.28	1.17±0.29
135°	1.49±0.38	1.03±0.44

Using the data of Walker[19] and Tollestrup[20] for values of $\sigma_0(\theta)$ and our measurements of R, the values of $P\alpha$ can be computed. The results are summarized in Table II. Note that since only ratios of the cross sections are of interest, only the errors in relative value rather than in absolute value need be considered. The errors in Tables II and III depend primarily on counting statistics.

It will be argued that if $P\alpha$ values at 45° differ significantly from those at 135°, an assumption that only S and P waves contribute is incorrect and that this indicates the need to introduce higher angular momenta. The degree of significance of this difference is determined by assuming $P\alpha_{45°}$ equal to $P\alpha_{135°}$ and then calculating the probability of obtaining differences in $P\alpha$ values greater than or equal to those found in Table II. Analyzing each energy separately and making the above assumptions, it is found that there is less than a 2% probability at 342 MeV and less than a 0.10% probability at 373 MeV of obtaining differences in the $P\alpha$ values greater than or equal to those given in Table II. This is considered to be sufficiently convincing evidence that the difference between $P\alpha_{45°}$ and $P\alpha_{135°}$ is not just due to statistical fluctuations in the data. Prior to obtaining the data it was decided that the difference between the 45° and 135° points was of greatest significance and, hence, an analysis in terms of only these two angles is appropriate. If such a decision had not been made, it would be necessary to include the
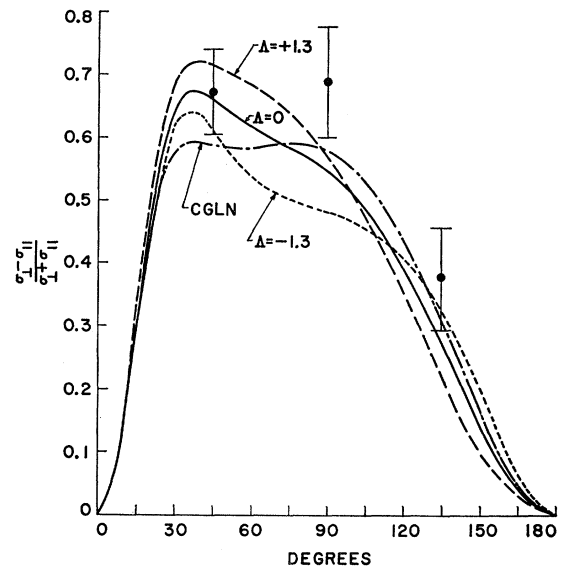

FIG. 10. Comparison of theoretical and measured values of $(\sigma_\perp - \sigma_{\shortparallel})/(\sigma_\perp + \sigma_{\shortparallel})$ at 359 MeV. The phase shifts of Table V are used and curves are shown for $\Lambda = 0$ and $\Lambda = \pm 1.3$. The CGLN (reference 5) predictions are shown for comparison.

[19] R. L. Walker, J. G. Teasdale, V. Z. Peterson, and J. I. Velte, Phys. Rev. 99, 210 (1955).

[20] A. V. Tollestrup, J. C. Keck, and R. M. Worlock, Phys. Rev. 99, 220 (1955).

90° data in the analysis and the test would not be statistically quite as convincing. A major advantage of the use of polarized x rays is that only two measurements are necessary. The known variation of meson photoproduction with energy also makes credible the assumption that $P\alpha$ does not undergo extreme fluctuations as a function of energy. With this assumption the fact that the measured values of the ratio at 45° are greater than the ratio at 135° at both energies takes on statistical significance.

In the above analysis, use has been made of the assumption that the polarization does not vary from one run to another. A more general analysis, considering that the polarization remains constant during one data run but making no assumptions as to the behavior of the polarization from one run to another, can be made. This analysis was made by calculating an "expected" value of $P\alpha_{45°}$ and $P\alpha_{135°}$ for each separate data run by making a least-squares fit to the data. A χ^2 test is then applied to these expected values of $P\alpha_{45°}$ and $P\alpha_{135°}$ for each separate data run. Making use of the reproductive property of the χ^2 distribution the values of χ^2 for each separate data run are summed to give a total χ^2 value for all runs at each energy. The results of this statistical analysis at 373 and 342 MeV show that, on a repeated series of measurements, there would be less that a 2% probability of obtaining fluctuations from the expected $P\alpha$ values greater than those obtained. Again this is considered to be sufficiently convincing evidence that the difference between $P\alpha_{45°}$ and $P\alpha_{135°}$ is not just due to the statistical fluctuations in the data. It is recognized, in applying the χ^2 test to the $P\alpha$ values, that $P\alpha$ is not a normal distribution. However,
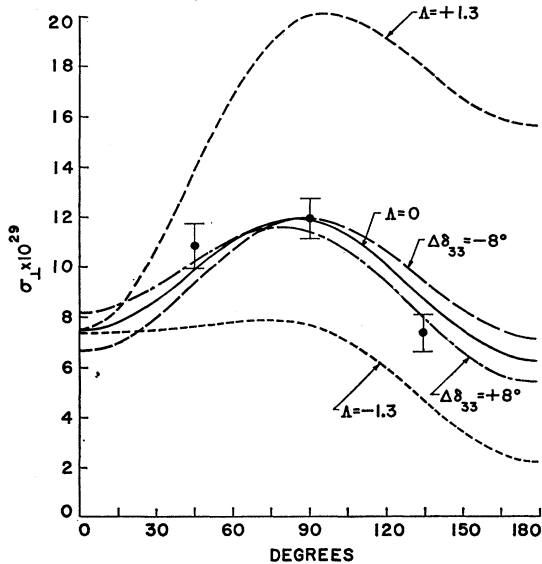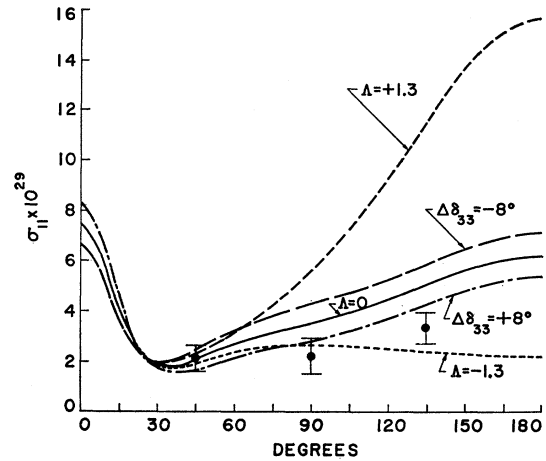

FIG. 12. Comparison of theoretical and measured values of σ_{II} at 359 MeV. Curves show the effects of varying Λ while using the phase-shift values of Table V and also the effects of varying δ_{33} by $\pm 8°$ with $\Lambda = 0$.

for the values of interest this non-normality is small and introduces negligible error in the χ^2 test.

It is perhaps worth emphasizing again that this analysis is independent of any nonphenomenological knowledge of meson physics or of any assumptions concerning the polarization with the exception of our assertion that we are capable of keeping the polarization constant during each separate data run.

Data taken at lower energies of 227 and 240 MeV, (shown in Table III), where the polarization and, hence, the ratio is smaller, are not accurate enough to allow as convincing an argument as at the higher energies.

This is due to the fact that $P\alpha$ is proportional to $(R-1)/(R+1)$; and therefore, the error in $P\alpha$ is proportional to $2\Delta R/(R^2-1)$, where ΔR is the error in the ratio R. Thus, the fractional error in $P\alpha$ becomes large as R approaches one.

In addition, one would expect that the closer the photon energy is to threshold, the more probable it would be that the data could be fit without the retardation term. Analyzing the low-energy data assuming the same polarization in all runs, it was found that there is a 70% probability at 227 MeV and a 9% probability at 240 MeV of obtaining differences in $P\alpha$ values greater than or equal to those given in Table III. It should be noted that for both low energies $P\alpha_{45°}$ is

FIG. 11. Comparison of theoretical and measured values of $\sigma_{\perp}$ at 359 MeV. Curves show the effects of varying Λ while using the phase-shift values of Table V and also the effects of varying δ_{33} by $\pm 8°$ with $\Lambda = 0$.

TABLE III. Measured values of $[-\sigma_0(\theta)/\sin^2\theta](R-1)/(R+1)$ at 227 and 240 MeV. These values should be independent of angle if only S and P waves are present.

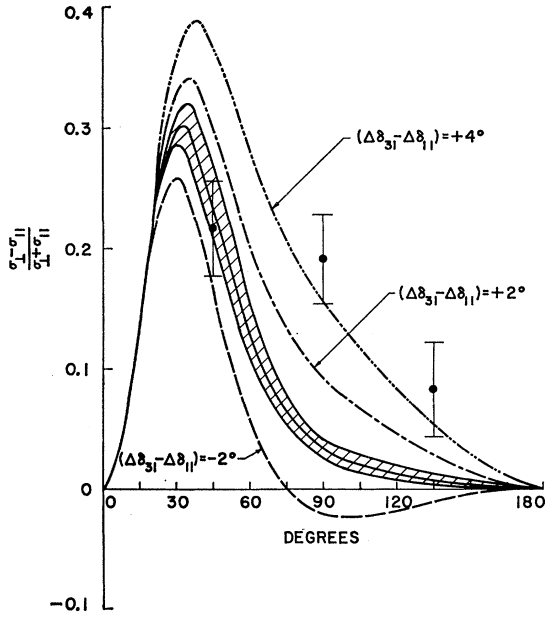|	$\dfrac{-\sigma_0(\theta)}{\sin^2\theta}\left(\dfrac{R-1}{R+1}\right)_{k=227 \text{ MeV}}$ (μb/sr)	$\dfrac{-\sigma_0(\theta)}{\sin^2\theta}\left(\dfrac{R-1}{R+1}\right)_{k=240 \text{ MeV}}$ (μb/sr)
45°	0.90±0.24	0.97±0.29
90°	0.73±0.17	0.54±0.21
135°	0.77±0.31	0.07±0.44

FIG. 13. Comparison of theoretical and measured values of $(\sigma_\perp - \sigma_{||})/(\sigma_\perp + \sigma_{||})$ at 234 MeV. In all curves $\Lambda = 0$. The central band encompasses the effects of varying δ_1, δ_3, δ_{13}, and δ_{33} individually by $\pm 2°$ from the values of Table V. Other curves show the effects of varying δ_{31} and δ_{11} which appear together in the dispersion theoretical calculations.

larger than $P\alpha_{135°}$ as was the case for the high-energy data.

Thus, the low-energy data, while not itself conclusive, tend to substantiate the conclusions obtained using the high-energy data. The more general analysis applied to this low-energy data does not yield statistically significant conclusions.

Some of the data were taken with peak bremsstrahlung energies above pion-pair threshold, so corrections for pair production must be made but since the amount of asymmetry in pion pair production is not known, exact correction is not possible. However, it can be argued that the pair production corrections, although unknown in magnitude, are of such a sign that they would increase the difference between $P\alpha_{45°}$ and $P\alpha_{135°}$ if applied.

This argument makes use of the fact that since the pair production of interest is just slightly above pair threshold, the extra pion adds a pseudoscalar to the reaction. Thus, it can be shown that the effect of pion pairs is to reduce the measured ratio, and that a pion-pair correction if applied would increase the ratio. No corrections need to be made to the 135° data since it was kinematically impossible to have pion pair contamination at this angle. Corrections need be made only to the 45° data and from the above argument would be such as to increase the ratio, R, at 45°. The data in Table I, thus, give a lower limit of this difference. Best

[21] M. Bloch and M. Sands, Phys. Rev. 113, 305 (1959).

estimates of the magnitude of the pair correction, using Bloch and Sands[21] data and May's values of the polarization, give less than a 2% correction. The small value of this correction is to be expected because pair production is caused by higher energy photons which would have a lower polarization.

It is possible to attempt to draw further conclusions from the data in Tables II and III. Under the assumption of S, P, and $D_{3/2}$ or S, P, and a small amount of D wave contribution to the photoproduction amplitude, the cross section was shown to be of the form:

$$\sigma = \sigma_0 + (\alpha + \beta \cos\theta) \sin^2\theta \cos 2\varphi. \quad (9)$$

An equation analogous to Eq. (14) can be found:

$$-P(\alpha + \beta \cos\theta) = \frac{\sigma_0(\theta)}{\sin^2\theta}\left(\frac{R-1}{R+1}\right). \quad (23)$$

For use of the above equation, Table II is now considered to list values of $P(\alpha + \beta \cos\theta)$ rather than $P\alpha$ values. Let the measured values of $[\sigma_0(\theta)/\sin^2\theta] \times (R-1)/(R+1)$ at 45°, 90°, and 135° be labeled a, b, and c, respectively. Equation (15), using this notation, gives:

$$-P[\alpha + (1/\sqrt{2})\beta] = a, \quad (24)$$

$$-P(\alpha) = b, \quad (25)$$

and

$$-P[\alpha - (1/\sqrt{2})\beta] = c. \quad (26)$$

Using Eqs. (24)–(26) and the values of a, b, and c from Table II, the "expected" values of $P\alpha$ and
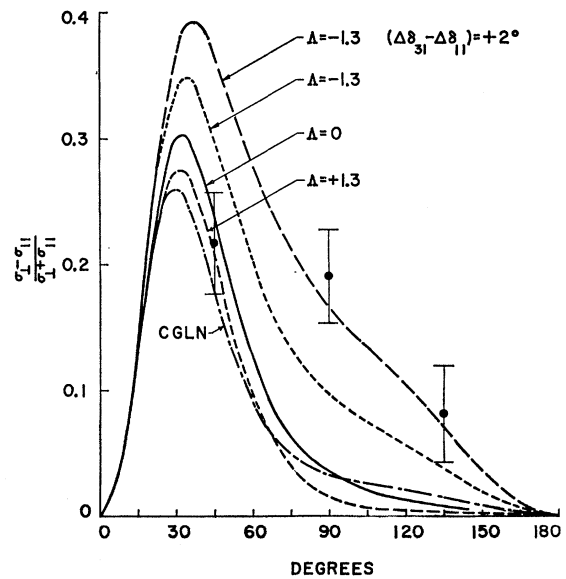

FIG. 14. Comparison of theoretical and measured values of $(\sigma_\perp - \sigma_{||})/(\sigma_\perp + \sigma_{||})$ at 234 MeV. Curves are shown for $\Lambda = 0$ and $\Lambda = \pm 1.3$ using the phase-shift values given in Table V. The predictions of CGLN are shown for comparison. A curve also shows McKinley's calculations with $\Lambda = 1.3$ and $\Delta\delta_{31} - \Delta\delta_{11} = +2°$.

$(1/\sqrt{2})P\beta$ can be calculated by making a least-squares fit to the data. These expected values are given in Table IV. A χ^2 analysis comparing the expected values of $P\alpha$ and $(1/\sqrt{2})P\beta$ from Table IV with the measured values of a, b, and c given in Table II gives an 11% probability for obtaining fluctuations as great or greater than those obtained.

It should be noted that the χ^2 test does not recognize the fact that in the data the ratio at 45° is always greater than the ratio at 135°. As mentioned above, this fact is significant if one assumes that $[\sigma_0(\theta)/\sin^2\theta]$ $\times(R-1)/(R+1)$ varies slowly with energy. Making this assumption fixes the direction of fluctuation for each measurement after the first, and thus, in this case reduces the probability even more.

Although this evidence is not conclusive, it is an indication that the addition of $D_{3/2}$ waves or a small amount of D wave to the phenomenological analysis is not sufficient to fit the data.

With the addition of the higher angular momentum states caused by a phenomenological addition of the retardation term it is apparent that a satisfactory fit to the data can be made.

These results are strong evidence for the necessity of including higher angular momentum states. In particular, very general theoretical considerations indicate that except for the retardation term, the number of angular momentum states are limited by the energy
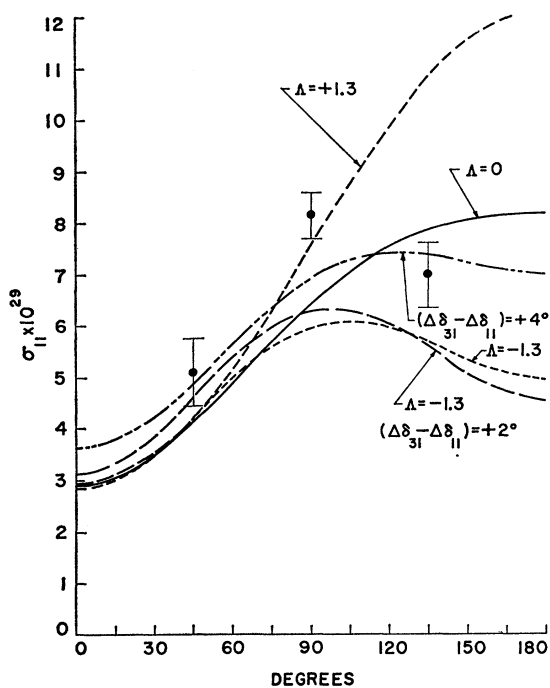

FIG. 16. Comparison of theoretical and measured values of $\sigma_{\perp\perp}$ at 234 MeV. Curves show the effects of varying Λ while using the phase-shift values of Table V. A curve also shows the predicted values with $\Lambda=0$ and $\Delta\delta_{31}-\Delta\delta_{11}=+4°$ and another curve shows the predictions with $\Lambda=-1.3$ and $\Delta\delta_{31}-\Delta\delta_{11}=+2°$.

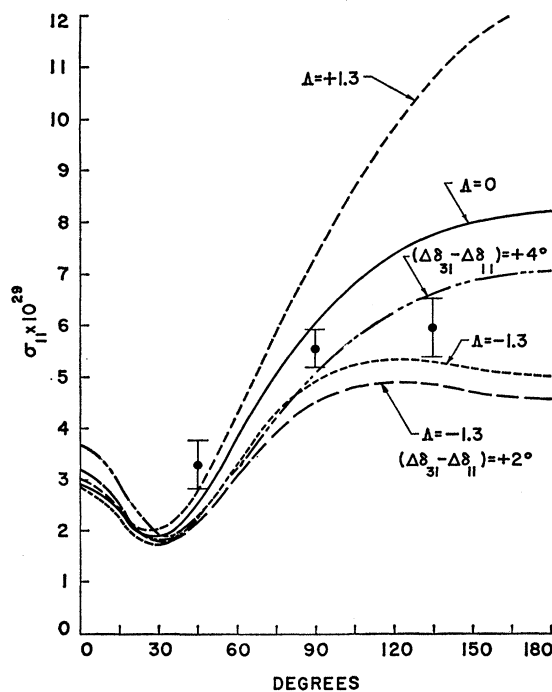of the outgoing meson and, hence, through the kinematics of the reaction, by the energy of the incident photon. Therefore, the failure of the phenomenological analysis to agree with the data, unless we include higher angular momenta which are improbable or the retardation term, is an indication that the retardation term

TABLE IV. Measured value of $-P\alpha$ and $-(1/\sqrt{2})P\beta$ at 342 and 373 MeV. These values should be the same if only S, P, and $D_{3/2}$ waves or S, P, and a small amount of D wave are present.

	$k=342$ MeV	$k=373$ MeV
$-P\alpha$	1.98	1.58
$-(1/\sqrt{2})P\beta$	0.61	1.01

is necessary for the analysis of charged meson photoproduction.

A comparison of our results with the predictions of the relativistic dispersion relation unfortunately is difficult since not only may there be basic difficulties from inaccuracies due to the evaluation of dispersion integrals over the unobservable and high-energy regions but the phase shifts used in the calculations are not well established.

Here again we use the work of McKinley[4] who has fitted existing analyzed phase shifts with polynomials encompassing an energy range between 0- and 600-MeV pion energy. Although, as McKinley points out, this

FIG. 15. Comparison of theoretical and measured values of $\sigma_{\perp}$ at 234 MeV. Curves show the effects of varying Λ while using the phase-shift values of Table V. A curve also shows the predicted values with $\Lambda=0$ and $\Delta\delta_{31}-\Delta\delta_{11}=+4°$ and another curve shows the predictions with $\Lambda=-1.3$ and $\Delta\delta_{31}-\Delta\delta_{11}=+2°$.

TABLE V. Values of the phase shifts used in these calculations.

		δ_1	δ_3	δ_{11}	δ_{13}	δ_{31}	δ_{33}
Photon energy	234	8.1	−7.8	−0.6	−0.2	−2.0	14.7
in MeV	359	13.4	−17.2	−0.1	−1.0	−3.9	99.8

method does not take into account correlations between different phase shifts, it is the only analysis which covers a large energy range and all existing data. As such it appears very useful and we elect to use it here. It is, however, impossible to determine the accuracy of such a treatment, and hence, in our data we somewhat arbitrarily show curves allowing an overly generous ±2° variation of the individual phase shifts for the low-energy pions and ±2° variation of the small phase shifts and ±8° variation of the δ_{33} phase shift near the resonance energy.

The phase-shift values obtained from McKinley's formulas are listed in Table V. In our comparisons with theory we have used a 234-MeV average of our low-energy data and a 359-MeV average of the high.

The fundamental comparison of our data with McKinley's calculations is given in Figs. 9–16.

Figure 9 is for 359 MeV and the γ, ρ, π coupling parameter $\Lambda = 0$. The effects of varying the small phase shifts by ±2° individually is shown by the shaded area. Two other curves show the effect of a ±8° variation of the δ_{33} phase shift.

Figure 10 shows the effect of varying the value of Λ. In all these curves the central value of the phase shifts is used. The CGLN prediction is given for comparison.

It can be seen that the asymmetry value is relatively insensitive to these variations and that our data are in good agreement with the predictions of the McKinley theory.

Figures 11 and 12 show values of $\sigma_\perp$ and $\sigma_\parallel$. Here we combine our data with the values measured with unpolarized bremsstrahlung.[19,20] Any conclusions here are more sensitive to the unpolarized cross sections than to the asymmetry effects. The simple form of Fig. 11 is due to the absence of the meson current term.

Figures 13 and 14 give asymmetry comparisons for the lower energy points. In Fig. 13 the effects of a variation of the phase shifts are shown. The central band shows the effects of varying δ_1, δ_3, δ_{13}, and δ_{33} by ±2°. Although the asymmetry is insensitive to this variation, it is affected by a variation in δ_{11} or δ_{31}. In the CGLN theory these are always in a combination $\delta_{31} - \delta_{11}$ and, hence, a variation gives an effect different only in sign. The McKinley theory changes this in only a minor way. A major variation, $\Delta(\delta_{31} - \delta_{11}) = +4°$ is necessary to make the 90° point fit but this in turn raises the value too much at 45°. Figure 14 shows the effect of introducing the ρ. Any reasonable value of Λ cannot bring this into agreement with our data although we do seem to favor a negative value. A change of the δ_{11} and δ_{31} phase shifts might be suggested but no combination would appear to be a good fit. It should be pointed out that ±2° variations are much more than any reasonable analysis of the small phase shifts would appear to allow. Again $\sigma_\perp$ and $\sigma_\parallel$ are shown in Figs. 15 and 16, and as before it is apparent that ρ effects are more easily seen in ordinary cross-section measurements.

To summarize, we come to the following conclusions. A phenomenological analysis of our data indicates the need of introducing higher angular momenta than S, P, and D waves. We interpret this as indicating the need to include a retardation term in our analysis. Our data are in excellent agreement with McKinley's predictions at 359 MeV but at 234 MeV no combinations of phase shifts or ρ coupling will make the agreement good. We appear to favor a negative value of Λ and values of δ_{11} more negative and δ_{31} more positive than predicted.

ACKNOWLEDGMENTS